J. Fluid Mech. (1978), *vol.* 84, *part* 4, *pp.* 609–624
Printed in Great Britain

Meandering and braiding of rivers

By JØRGEN FREDSØE

Institute of Hydrodynamics and Hydraulic Engineering, Technical University of Denmark, DK 2800 Lyngby/Copenhagen

(Received 6 January 1977)

The origin of meandering and braiding of alluvial rivers is re-analysed in terms of stability theory. The flow is described by a two-dimensional model, and the transportation of sediment is separated into bed-load transport and transport of suspended sediment, by use of the improved knowledge of sediment transport mechanisms achieved in recent years. The paper explains why it is important to distinguish between the sediment transported as bed load and that in suspension.

The analysis is able to predict whether a river remains stable or tends to meander or braid.

The results of the stability analysis are compared with laboratory experiments and data from natural rivers, and the agreement is satisfactory.

1. Introduction

The instability of rivers has been investigated theoretically by several authors during the last decade. Of the great number of publications, the contributions by Hansen (1967), Callander (1969) and Engelund & Skovgaard (1973) should be mentioned because of their relevance to the present paper.

Hansen and Callander both applied a two-dimensional flow model, assuming that the direction of the local sediment transport is parallel to the local velocity vector and that the sediment transport rate is uniquely related to the bed shear stress.

Engelund & Skovgaard extended the analysis by introducing a three-dimensional flow model which takes account of the helical motion induced because of the non-uniform vertical velocity distribution in the basic flow, an effect neglected in the previous approaches. Further, they introduced the effect of a transverse bed slope on the transportation of the sediment and found that this effect is of great significance, because the theory predicts that the river will braid into an infinite number of branches if it is not included. This suggests that an accurate knowledge of the interaction of fluid flow and sediment motion is necessary in order to develop an adequate description of the river instability.

In the present paper the flow is described by essentially the same two-dimensional, linearized flow model as was adopted by Hansen, Callander and recently by Parker (1976). The theory differs from the previous one in the following respects:

(i) The linearized equations are solved numerically without introducing further approximations, such as the perturbation methods applied by Parker and to some extent by Callander. This point seems to be more important than has been realized previously.

(ii) The effect of a transverse slope of the bed is accounted for. During the last few years this problem has been investigated in a number of publications and a preliminary solution has obtained a considerable amount of theoretical and experimental support. As mentioned above, this particular effect is very important in the analysis.

(iii) The total amount of sediment is transported partly as bed load and partly in suspension. The fact that at large flow rates a greater part of the sediment load will be carried in suspension implies that there can be no unique relationship between the transport rate and the bed shear stress. To account for this it is necessary to introduce a supplementary equation of continuity for the suspended sediment, and to be able to estimate the transport rates of the bed load and the suspension separately.

2. Derivation of the linearized flow equations

As in many previous investigations, the formation of meanders is related to the instability of an alluvial channel with fixed and impermeable side walls. As the migration velocity of the developing alternate bars is very small the flow is assumed to be quasi-steady.

The bed is assumed to be deformed by a doubly periodic perturbation h of the form

$$h = h_0 \cos(k_3 x_3) \exp(ik_1 x_1) = h_0 E. \tag{1}$$

Here x_1 is the co-ordinate in the flow direction, x_3 the transverse co-ordinate and k_1 and k_3 are the wavenumbers in these two directions. h_0 is the amplitude of the perturbation. The flow over this doubly periodic bed is described by the following two equations of motion:

$$U_1 \frac{\partial U_1}{\partial x_1} + U_3 \frac{\partial U_1}{\partial x_3} = gI_0 - \frac{\tau}{\rho y} - g \frac{\partial (h+y)}{\partial x_1}, \tag{2}$$

$$U_1 \frac{\partial U_3}{\partial x_1} + U_3 \frac{\partial U_3}{\partial x_3} = -\frac{U_3}{U_1} \frac{\tau}{\rho y} - g \frac{\partial (h+y)}{\partial x_1}, \tag{3}$$

where U_1 and U_3 are the velocity components in the x_1 and x_3 directions, y is the local water depth, g the acceleration due to gravity, ρ the density of water, I_0 the undisturbed slope of the channel and τ the local bed shear stress in the x_1 direction. Equations (2) and (3) are valid if the vertical accelerations of the fluid are neglected (hydrostatic pressure), if vertical variations of the velocity are neglected and if the tractive force on the bed has the direction of the velocity vector.

The equation of continuity for the water is

$$\frac{\partial}{\partial x_1}(U_1 y) + \frac{\partial}{\partial x_3}(U_3 y) = 0. \tag{4}$$

If we assume that the amplitude of the bed perturbation h_0 is small, it is possible to linearize (2)–(4) by introducing

$$U_1 = U + u_1, \quad U_3 = u_3, \quad y = D + \eta, \quad \tau = \tau_b + \tilde{\tau}, \tag{5}$$

where U is the flow velocity, D the depth and τ_b the bed shear stress in the unperturbed flow, while u_1, u_3, η and $\tilde{\tau}$ are small quantities.

Assuming that the perturbations are doubly periodic like the bed elevation, we may write

$$u_1 = u_{10} E, \quad \eta = \eta_0 E, \quad \tilde{\tau} = \tau_0 E, \quad u_3 = u_{30} \tan(k_3 x_3) E, \tag{6}$$

where E has been introduced in (1). Inserting (5) and (6) into (2)–(4) gives

$$Uik_1 u_{10} = \frac{\tau_b}{\rho D}\frac{\eta_0}{D} - \frac{\tau_0}{\rho D} - ik_1 g(h_0 + \eta_0), \tag{7}$$

$$Uik_1 u_{30} = -\frac{u_{30}}{U}\frac{\tau_b}{\rho D} + k_3 g(h_0 + \eta_0), \tag{8}$$

$$Uik_1 \eta_0 + Dik_1 u_{10} + Du_{30} k_3 = 0. \tag{9}$$

In order to solve these three equations, a relation between the shear stress and other hydraulic parameters is needed. Such a relation is usually given in the form

$$\frac{\tau_0}{\tau_b} = \alpha\frac{u_{10}}{U} + \beta\frac{\eta_0}{D} \tag{10}$$

as demonstrated in the next section, and by use of this relation, (7)–(9) can be transformed into the following dimensionless equations:

$$\frac{u_{10}}{U}(\mathscr{F}^2 ik_1 D + \alpha I_0) + \frac{\eta_0}{D}(ik_1 D + I_0(\beta - 1)) + \frac{h_0}{D} ik_1 D = 0, \tag{11}$$

$$\frac{u_{30}}{U}(\mathscr{F}^2 ik_1 D + I_0) - \frac{\eta_0}{D} k_3 D - \frac{h_0}{D} k_3 D = 0, \tag{12}$$

$$\frac{u_{10}}{U} ik_1 D + \frac{u_{30}}{U} k_3 D + \frac{\eta_0}{D} ik_1 D = 0, \tag{13}$$

in which $\mathscr{F} = U/(gD)^{\frac{1}{2}}$ is the Froude number. From (11)–(13) the flow field can be calculated for given hydraulic parameters.

3. Hydraulic resistance of alluvial channels

The variation of the friction factor with flow velocity is rather complicated because different bed forms (ripples, dunes, plane bed, standing waves or antidunes) exist for different flow conditions, so that the geometry of the bed changes with flow velocity.

(i) In case of a *dune-covered* bed, the resistance can be determined from the relation (Engelund & Hansen 1972)

$$\theta' = 0{\cdot}06 + 0{\cdot}4\theta'^2, \tag{14}$$

where θ is the Shields parameter and θ' the effective Shields parameter, i.e.

$$\theta = \tau/(s-1)gd, \quad \theta' = \theta y'/y, \tag{15}$$

in which s is the relative density and d the diameter of the grains. y' can be calculated from the following equation, suggested by Einstein (1950):

$$U/(gy'I)^{\frac{1}{2}} = 6 + 2{\cdot}5\ln(y'/k), \tag{16}$$

where k is the sand roughness, which Engelund & Hansen put equal to $2{\cdot}5d$. From (14)–(16) a relationship of the form given by (10) is obtained, with coefficients

$$\alpha = (0{\cdot}4\theta'^2/\theta' + (1 - 0{\cdot}8\theta'^2/\theta')\kappa)^{-1}, \quad \beta = \kappa\alpha, \tag{17}$$

in which κ is given by

$$\kappa = -2{\cdot}5[6 + 2{\cdot}5\ln(D'/2{\cdot}5\alpha)]^{-1}.$$

(ii) If the unperturbed bed is *plane*, the resistance can be calculated from (16) with $y' = y$ (no form drag). Now the constants in (10) are given by

$$\alpha = 2, \quad \beta = -5/[6 + 2{\cdot}5 \ln (D/2{\cdot}5\alpha)]^{-1}. \tag{18}$$

As *ripples* can be considered as roughness elements which do not change their geometry with the flow (see for instance Yalin (1972, p. 227), who states that the ripple length is equal to $1000d$), the constants in (10) will be determined by (18) in this case also.

4. Transportation of sediment as bed load and in suspension

As far as the formation of dunes and antidunes is concerned, it has been pointed out (Engelund 1971; Engelund & Fredsøe 1974) that it is necessary to distinguish between the sediment transported as bed load and sediment transported in suspension. In the above-mentioned papers the bed load is defined as that part of the total load which adapts to spatial changes in the tractive stress so that spatial lag may be neglected. It is important to distinguish between bed load and suspended load, because the suspended load responds with a certain lag caused by the fact that the particles have to settle a certain distance before they become deposited. This lag is able to explain the formation of antidunes, while the lag originating from the fluid friction, combined with sediment transported as bed load, can explain the formation of dunes. As the two above-mentioned lags in some sense counteract each other, the transition from dunes to a plane bed can be explained as depending on the ratio between the mean rate q_s of suspended load and the mean rate q_b of bed load (Engelund & Fredsøe 1974).

In the present analysis, a distinction between the bed load and the suspended load has been made for the following reasons. As far as the meander stability is concerned, the lag between bed and tractive stress caused by the fluid friction is rather small because of the large wavelengths. This may not generally be the case for the phase between the local tractive stress and the local transport of suspended sediment as this phase strongly depends on the value of the fall velocity of the suspended particles. This phase has been included in the present model by introducing the equation of continuity in three dimensions for the suspended sediment.

In addition, the discrimination between bed load and suspended load is important for reasons explained below.

In the simple model developed by Hansen, it was assumed that the sediment is transported in the direction of the local bed shear vector. However, this simple model leads to the conclusion that the river will tend to braid in an infinite number of branches. The same result was obtained in the more complete three-dimensional model by Engelund & Skovgaard. In order to explain this paradox, Engelund & Skovgaard introduced a correction term which took into account the effect of the transverse slope on the lateral sediment transport rate. Since their paper appeared, the information on this effect has been increased considerably.

The motion of a bed particle in a flow where the bed is sloping weakly in the transverse direction was treated theoretically by Engelund (1974), who found that

$$\tan (\psi - \delta) = \frac{-1}{\tan \Phi} \frac{\partial h}{\partial x_3} - \tan \delta, \tag{19}$$

where δ is the deviation of the bed shear direction from the x_1 direction and ψ the angle between the particle path and the bed shear stress. Φ is the dynamic friction angle.

Equation (19) was used by Engelund to calculate the bed topography in a meandering channel. The good agreement between theory and experiments supports the validity of (19). In a later theory concerning the instability of flow in an annular channel, Engelund (1975) again obtained experimental evidence in favour of this theory.

Further, Gottlieb (1976) and Fredsøe (1976) have tested the validity of (19). Gottlieb calculated the flow in a weakly meandering channel with fixed side walls and was able to calculate from (19) a form of the bed in good agreement with his experimental findings. Fredsøe calculated the sedimentation of river navigation channels, where the flow is parallel to the direction of the navigation channel, so that in this case the theory becomes particularly simple. Here the agreement between theory and experiment was very satisfactory.

In most of the above-mentioned experiments, the bed was covered either with ripples or with dunes, which does not seem to affect the validity of (19).

The main reason why it is necessary to distinguish between bed and suspended load is that the effect of the transverse slope acts on only the bed load, as the action of gravity on suspended particles has no transverse component. Because the effect of a transverse slope is rather significant, it is of importance to know the ratio q_b/q_s as accurately as possible. Much research has been done in order to solve this problem in connexion with sand-bed instability (Engelund & Fredsøe 1974; Fredsøe & Engelund 1975). In a recent paper Engelund & Fredsøe (1976) presented a new mathematical model of sediment transport in straight alluvial channels. This model is based on physical ideas related to those introduced by Bagnold (1954) and to experiments by Fernandéz Luque (1974). The paper predicts the bed load q_b to be given by

$$\Phi_b = q_b/[(s-1)gd^3]^{\frac{1}{2}} = 5p(\theta'^{\frac{1}{2}} - 0{\cdot}7\theta_c^{\frac{1}{2}}), \tag{20}$$

where θ_c is the critical Shields parameter and p is that fraction (= probability) of the particles in a single layer which is transported just above the immobile bed. For p the following expression was suggested:

$$p = \left[1 + \left(\frac{\frac{1}{6}\pi \tan \Phi}{\theta' - \theta_c}\right)^4\right]^{-\frac{1}{4}}. \tag{21}$$

Further, the model is able to predict the bed concentration c_a of the suspended material. This is given by

$$c_a = 0{\cdot}65/(1 + \lambda_a^{-1})^3, \tag{22}$$

where λ_a is the linear concentration at the bed level, given by

$$\lambda_a = \left(\frac{\theta' - \theta_c - \frac{1}{6}\pi \tan(\Phi)\, p}{0{\cdot}027 s\theta'}\right)^{\frac{1}{2}}. \tag{23}$$

The relation between c_a and θ' is sketched in figure 1 for given values of s and Φ. For large values of θ', c_a becomes constant and equal to 0·32, which seems to be a reasonable maximum value for suspended sediment in motion.

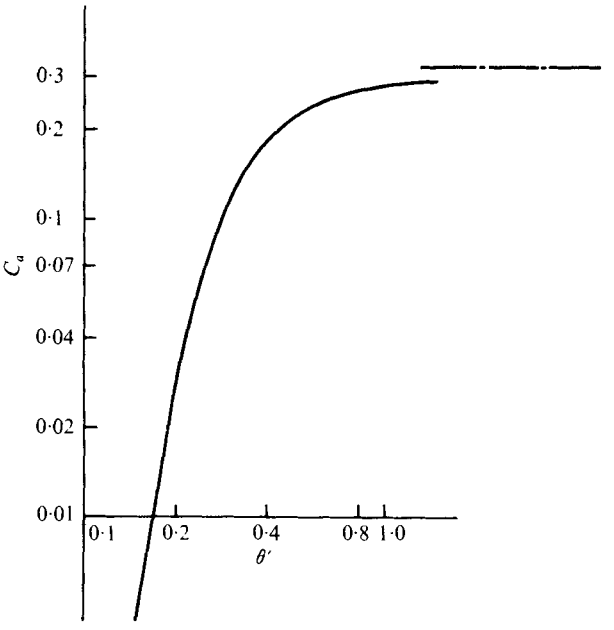

FIGURE 1. Variation in the bed concentration c_a of suspended sediment with θ'.

Assuming a parabolic distribution of the eddy viscosity, Rouse (1937) derived the following vertical distribution of the concentration of suspended material:

$$\frac{c}{c_a} = \left(\frac{y-x_2}{x_2}\frac{a}{y-a}\right)^{w/0{\cdot}4U_f'}, \tag{24}$$

where c_a is the concentration at $x_2 = a$ and w the fall velocity of sediment. The effective value of w is determined in the same way as in earlier investigations concerning dune instability (Engelund & Fredsøe 1974), by requiring that a particle goes into suspension if $w < 0{\cdot}8\,U_f'$. The transport rate q_s can be found from

$$q_s = \int_a^y c\,V\,dx_2, \tag{25}$$

V being the mean flow velocity at a distance x_2 from the bed. a is normally taken as $2d$.

By substituting (24) into (25), Einstein (1950) derived the following expression for the suspended load:

$$q_s = 11{\cdot}6c_a\,aU_f'[I_1 \ln(30y/k) + I_2], \tag{26}$$

where the constants I_1 and I_2 may be taken from the work charts published by Einstein.

The distribution of the suspended load in the non-uniform flow is expressed mathematically as an equilibrium between settling, diffusion and convection. In the present analysis, the calculations are simplified by neglecting vertical variations in the eddy viscosity. This leads to the so-called 'slip-velocity' model introduced by Engelund (1971). The equation of continuity for a unit volume of water–sediment mixture becomes

$$dc/dt = w\,\partial c/\partial x_2 + \epsilon\nabla^2 c, \tag{27}$$

where ϵ is the eddy-viscosity coefficient, given by $\epsilon = 0{\cdot}077\,U_f y$.

In the case of steady uniform flow, (27) reduces to a single ordinary differential equation with solution

$$c_0 = c_{b0} \exp(-wx_2/\epsilon), \tag{28}$$

where x_2 is the vertical co-ordinate and c_{b0} is a nominal concentration at the bed, which differs from that calculated from (22) and (23). The nominal bed concentration c_{b0} is determined by calculating the total suspended transport by the slip-velocity method and putting this result equal to the q_s obtained from (26).

In the perturbed flow we write the concentration as

$$c = c_0 + \tilde{c}, \tag{29}$$

where $\tilde{c}$ is a small quantity. On substituting (29) into (27) and linearizing, we obtain

$$U\frac{\partial \tilde{c}}{\partial x_1} + u_2 \frac{\partial c_0}{\partial x_2} = w\frac{\partial \tilde{c}}{\partial x_3} + \epsilon\left(\frac{\partial^2 \tilde{c}}{\partial x_1^2} + \frac{\partial^2 \tilde{c}}{\partial x_2^2} + \frac{\partial^2 \tilde{c}}{\partial x_3^2}\right), \tag{30}$$

in which the vertical flow velocity has been neglected to be consistent with the application of a two-dimensional flow model.

If we write the perturbation of the concentration profile as

$$c = \phi(x_2/D)\, E, \tag{31}$$

(30) becomes

$$\phi'' + \frac{wD}{\epsilon}\phi' - \left(i\frac{Uk_1 D^2}{\epsilon} + (k_1 D)^2 + (k_3 D)^2\right) = -\frac{UDwDik_1 c_0 h_0}{\epsilon^2}. \tag{32}$$

This is an ordinary second-order differential equation with constant coefficients and its solution contains two unknown constants, which are determined by two boundary conditions:

(i) The vertical sediment flux must vanish at the surface, which yields

$$\epsilon\,\partial\tilde{c}/\partial x_2 + w\tilde{c} = 0 \quad \text{at} \quad x_2 = y,$$

or

$$\phi'(1) + (wD/\epsilon)\,\phi(1) = 0. \tag{33}$$

(ii) The variation in the correct value c_a of the bed concentration with the local flow conditions can be calculated from (22) and (23) to be given by

$$dc_a/d\theta = f(\theta')\, c_a\, d\theta'/d\theta, \tag{34}$$

where

$$f(\theta) = \frac{3}{2(\lambda_a^3 + \lambda_a^2)\, 0{\cdot}027s}\left\{\frac{\theta_c}{\theta^2} - \frac{\pi}{6}\tan\Phi\,\frac{\theta\,\partial p/\partial\theta - p}{\theta^2}\right\},$$

in which

$$\frac{\partial p}{\partial \theta} = \frac{(\frac{1}{6}\pi\tan\Phi)^4}{(\theta-\theta_c)^5}\, p^5. \tag{35}$$

To obtain the variation in the nominal bed concentration c_{b0} we now use the definition of c_{b0}, which is

$$q_s = \int_0^D U c_{b0} \exp\left(\frac{w}{\epsilon}x_2\right) \simeq U\frac{\epsilon}{w}c_{b0}\left[1 - \exp\left(-\frac{wD}{\epsilon}\right)\right], \tag{36}$$

where q_s is given by (26). This yields a relation between c_{b0} and c_a of the form

$$c_a U_f' = K c_{b0} U,$$

where K is a constant. By differentiating this expression with respect to θ, we obtain

$$\frac{1}{c_a}\frac{dc_a}{d\theta} = \frac{U_f'}{U}\frac{d}{d\theta}\left(\frac{U}{U_f'}\right) + \frac{1}{c_{b0}}\frac{dc_{b0}}{d\theta}. \tag{37}$$

From (16) it is easily shown that the first term on the right-hand side is always negligible. Hence (37) leads to the following boundary condition at the bed:

$$c_b = c_{b0} + h\frac{dc_0}{dx_2} + \tilde{c} = c_{b0}\left(1 + \theta f(\theta')\frac{d\theta'}{d\theta}\frac{\tilde{\tau}}{\tau_0}\right),$$

which yields

$$\phi(0) = c_{b0}\left(\frac{w^D}{\epsilon} + \theta f(\theta')\frac{d\theta'}{d\theta}\frac{\tau_0}{\tau_b}\right). \tag{38}$$

From the two boundary conditions (35) and (38), the function ϕ is easily calculated from (32).

5. The stability analysis

Having obtained the distribution of suspended load in the non-uniform flow, it is easy to carry out the stability analysis. To this end we consider the equation of continuity for the sediment

$$\frac{\partial q_1}{\partial x_1} + \frac{\partial q_3}{\partial x_3} = -(1-n)\frac{\partial h}{\partial t}, \tag{39}$$

where q_1 and q_3 are the total volumetric sediment transport rates per unit width in the x_1 and x_3 directions, respectively, and n is the porosity of the sand. Until now, the flow over a stationary bed has been considered. This description is allowed because the perturbation to the bed migrates very slowly, but, in fact, the perturbation to the bed given by (1) should be changed by writing the factor E as

$$E = \cos(k_3 x_3)\exp[ik_1(x_1 - at)], \tag{40}$$

where $a = a_r + ia_i$ is the complex migration velocity of the bed perturbation, which can be found from (39). The total transport q is the sum of the bed load and the suspended load. From (20) we find

$$\frac{\partial q_{b1}}{\partial x_1} = [(s-1)gd^3]^{\frac{1}{2}}\frac{\partial \Phi_{b1}}{\partial x_1} = q_b g(\theta')\frac{\partial \theta'}{\partial x_1}, \tag{41}$$

in which

$$g(\theta) = \frac{(\frac{1}{6}\pi\tan\Phi)^4}{(\theta-\theta_c)^5}\left\{1 + \left(\frac{\frac{1}{6}\pi\tan\Phi}{\theta-\theta_c}\right)^4\right\}^{-1} + \frac{1}{2\theta^{\frac{1}{2}}(\theta^{\frac{1}{2}} - 0{\cdot}7\theta_c^{\frac{1}{2}})}. \tag{42}$$

The local direction of bed-load transport deviates from the local direction of the bed shear stress according to (19), from which we obtain

$$q_{b3} = q_b\left\{\frac{u_3}{U} - \frac{1}{\tan\Phi}\frac{\partial h}{\partial x_3}\right\}. \tag{43}$$

Hence

$$\frac{\partial q_{b3}}{\partial x_3} = q_b\left\{k_3 D\frac{u_{30}}{U} + \frac{(k_3 D)^2}{\tan\Phi}\right\}E. \tag{44}$$

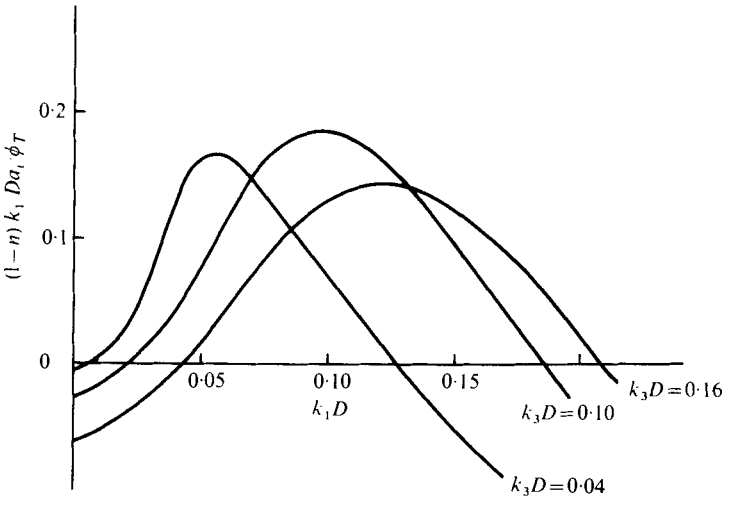

FIGURE 2. Variation in the amplification factor A with $k_1 D$ and $k_3 D$. $\theta = 0{\cdot}2$, $s = 2{\cdot}65$ and $c_D = 7$.

The longitudinal transport of suspended sediment is found from the expression

$$q_{s1} = \int_h^D (U + u_1)(c_0 + \tilde{c})\, dx_2. \tag{45}$$

By linearization we obtain

$$q_{s1} = -hc_{b0}\, U + q_{s0} + EUDG, \tag{46}$$

where

$$G = \int_0^1 \left[\phi + \frac{u_{10}}{U} c_{b0} \exp\left(-\frac{wD}{\epsilon}\frac{x_2}{D}\right)\right] d\left(\frac{x_2}{D}\right) \tag{47}$$

is easily obtained. The longitudinal variation in q_{s1} can now be calculated from (46). The transverse rate of transport of suspended sediment is given by

$$q_{s3} = \int_h^D u_3(c_0 + \tilde{c})\, dx_2 = q_{s0}\frac{u_{30}}{U} E. \tag{48}$$

By inserting (41), (44), (45) and (48) into (39), the complex migration velocity a can be calculated.

By use of the relations

$$I = (U_f/U)^2 \mathscr{F}^2$$

and

$$\frac{wD}{\epsilon} = 13\frac{w}{U_f} = 13\left(\frac{4(s-1)gd}{3c_D U_f^2}\right)^{\frac{1}{2}} = 13\left(\frac{4}{3\theta c_D}\right)^{\frac{1}{2}},$$

where c_D is the drag coefficient of the grains, it is possible to determine the migration velocity a as a function of a number of non-dimensional quantities:

$$a = a(\theta, c_D, s, D/d, k_1 D, k_3 D). \tag{49}$$

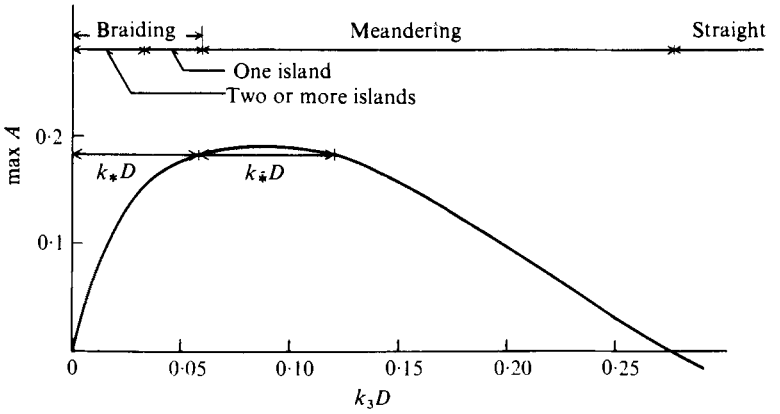

FIGURE 3. Variation in the maximum amplification factor with $k_3 D$. Parameter values as in figure 2.

6. Theoretical results

Having obtained the complex migration velocity a, it is now possible to work out stability diagrams: if $a_i > 0$ the flow is unstable, as the perturbation grows exponentially with amplification factor $k_1 D a_i$ [cf. (40)]. For given values of s, D/d and θ representative examples of the variation in the amplification factor with the parameters $k_1 D$, $k_3 D$ and θ are shown in figure 2. In this figure the amplification factor is normalized by the factor $(1-n)/\Phi_T$, where Φ_T is the total dimensionless rate of sediment transport. The figure shows that, for a given value of $k_3 D$, the amplification factor has a maximum value for a given $k_1 D$. This maximum determines the wavelength of the developing meander (Callander 1969; Hansen 1967). Further, if we plot this maximum value for different values of $k_3 D$, we obtain the characteristic variation in $\max A$ sketched in figure 3. From this it is seen that, if $k_3 D$ exceeds a critical value, $\max A$ becomes negative, and the river is stable (i.e. will remain straight). Further, if $k_3 D$ is smaller than that critical value, three-dimensional bars will be formed at the bed. If $k_3 D$ is smaller than a certain value $k_* D$, the amplification factor is greater at $(k_3 D)^* = 2k_3 D$, and the river will braid (Engelund & Skovgaard 1973). In this way it is possible to construct a stability diagram such as that sketched in figure 4, assuming that the bed is dune-covered. The figure shows at which values of $k_3 D = \pi D/B$ the river will remain straight, meander or braid as a function of θ. Here B is the width of the river. The lower dotted line in the figure indicates the transition from one to two braids. It must be mentioned that this stability diagram is very insensitive to changes in D/d, s and C_D. The influence of the sediment in suspension is seen by comparing figure 4 with figure 5, which shows the results of the stability theory incorporating bed load alone. It is seen that the stability limits have changed significantly: if the suspension is neglected, the bed will remain stable if θ is greater than about one.

The effect of the dunes on the river bed can be seen from figure 6, where a stability diagram has been constructed under the assumption that the unperturbed bed is plane. This yields stability limits which differ significantly from those presented in figure 4. At high values of θ it could be expected that the theory would predict a greater tendency towards braiding as it is the effect of the transverse slope on the bed load

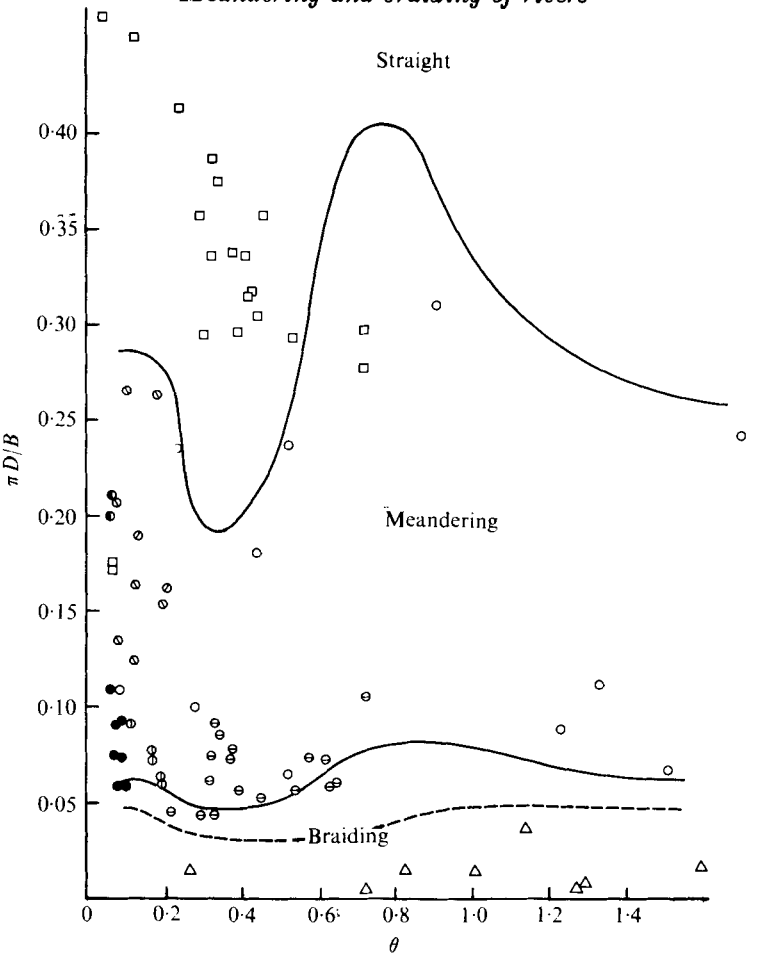

FIGURE 4. Stability diagram for a dune-covered river. $s = 2{\cdot}65$, $D/d = 1000$ and $c_D = 7$. The rectangles indicate straight data, the circles meandering and the triangles braiding. ⊖, Ackers & Charlton (1970); □, Shen & Komura (1968); ⓘ, □, Schumm & Khan (1972); ◐, Ashnida & Narai (1969); ●, Callander (1969); ⊘, Friedkin (1945); ⊘, Leopold & Wolman (1957); ○, △, data from rivers (Einstein & Barbarossa 1951; Schumm 1969; Hubbel & Matejka 1959; Danish rivers, The Danish Heath Society and B. Hasholt, Geografisk Institut, University of Copenhagen, unpublished).

which prevents infinite braiding, and the ratio q_s/q_b is increasing with θ. However, at large values of θ, c_b becomes constant as shown in figure 1, which implies that though the amount of suspended sediment is rather large the variation in q_s remains moderate.

In figures 7 and 8 the predicted value of the longitudinal wavenumber is shown as a function of $k_3 D$ and θ. In figure 7 the bed is assumed to be dune-covered, while the bed is plane in figure 8.

7. Comparison with experiments

Many experiments have been carried out in laboratory flumes in order to investigate the formation of meanders. These experiments have one advantage compared with data from nature: in nature the water discharge can vary quite a lot during a year,

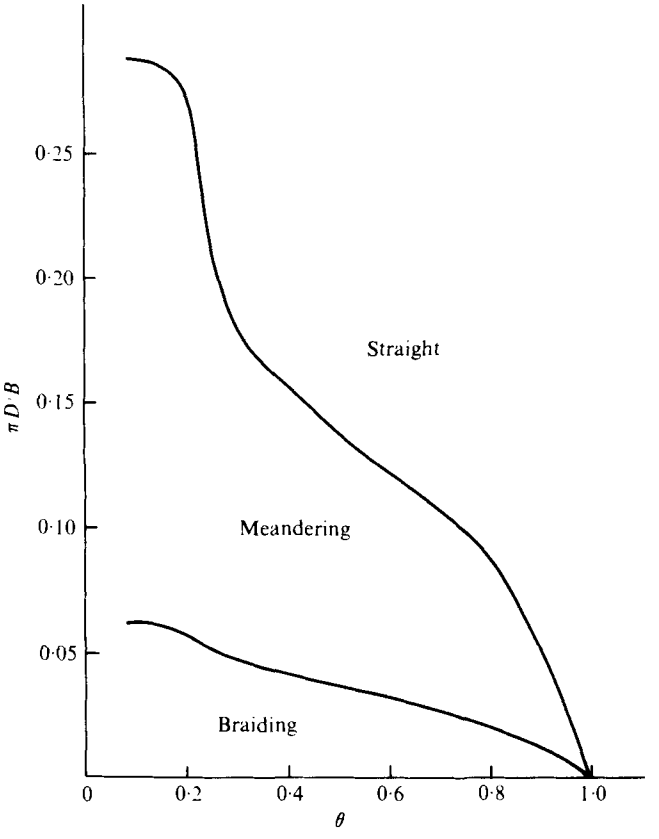

FIGURE 5. Stability diagram for a dune-covered bed where the suspended load has been neglected. $s = 2{\cdot}56$, $D/d = 1000$ and $c_D = 7$.

so that a formative discharge must be selected in order to compare observations with the theory. This formative discharge is close to the maximum discharge (bank-full discharge), for which the main part of the sediment transport takes place. In a laboratory flume the flow conditions are controlled, so that no difficulties concerning the formative discharge arise. However, in the laboratory a scale effect must be expected to take place, especially in experiments with small water depths. This scale effect is associated with the bed forms, because ripples or a plane bed will often be present instead of dunes. In their experiments Chang, Simons & Woolhiser (1971), for instance, do not mention the existence of dunes or ripples, and from their description of the bed it seems that the alternate bar pattern existed without any dunes or ripples superposed. Hence their data are plotted on the stability diagram in figure 6 for a plane bed, and the agreement is good, especially as regards the upper limit of the width–depth ratio at which alternate bars will develop. In their paper Chang *et al.* state that no alternate bar pattern could be observed if this ratio was lower than 12, which is the same as $k_3 D = 0{\cdot}26$.

In the same diagram some of the data from the paper by Schumm & Khan (1972) are depicted. Also here we have the problem concerning the behaviour of the bed form, but in those of the data where the Froude number exceeds 0·8, a plane bed

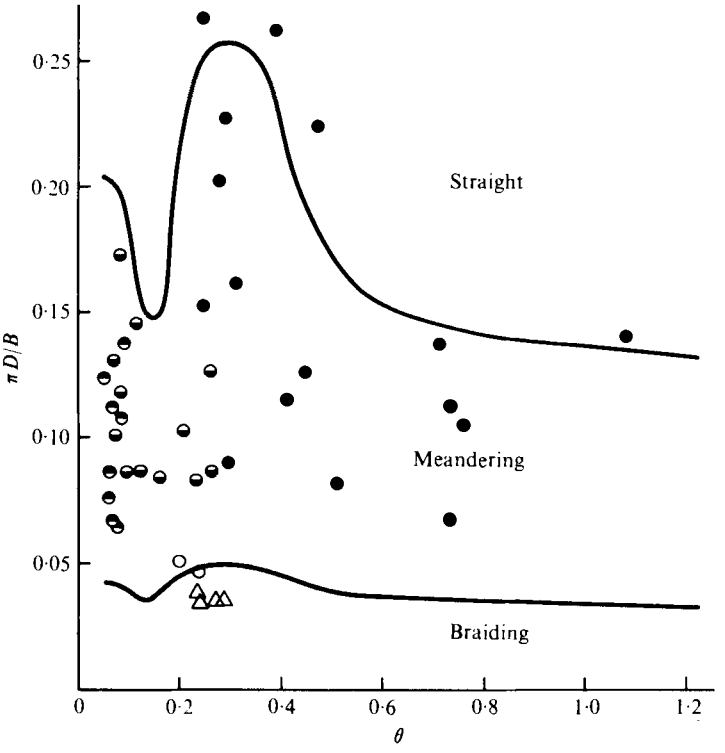

FIGURE 6. Stability diagram for an originally plane bed. The circles indicate meandering, the triangles braiding. $s = 2{\cdot}65$, $D/d = 1000$ and $c_D = 7$. ●, Chang *et al.* (1971), plastic pellets; ◒, Chang *et al.* (1971), clay; ◓, Chang *et al.* (1971), sand; ○, △, Schumm & Khan (1972).

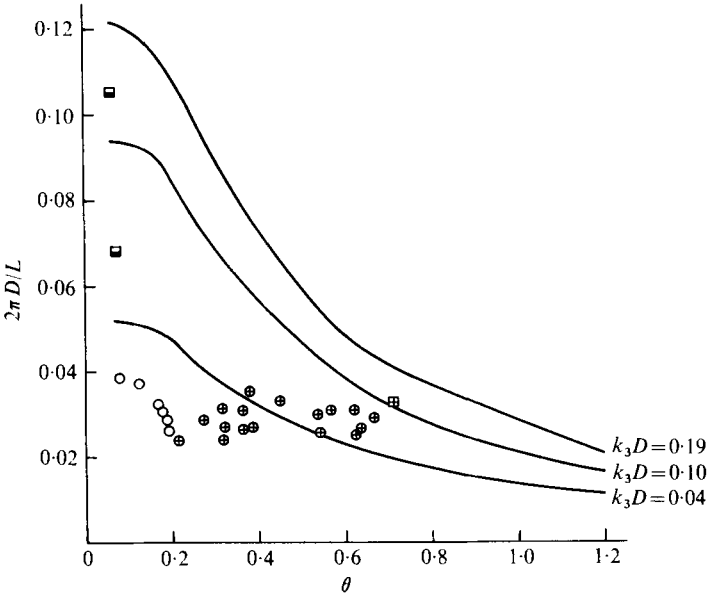

FIGURE 7. Comparison of predicted and longitudinal length of meanders for a dune-covered bed. The circles indicate data between the limits $0{\cdot}04 < k_3D < 0{\cdot}1$, while the rectangles indicate data for which $k_3D > 0{\cdot}1$, $s = 2{\cdot}65$, $D/d = 1000$ and $c_D = 7$. ○, Schumm (1969); ⊕, ⊞, Ackers & Charlton (1970); □, Ashnida & Narai (1969).

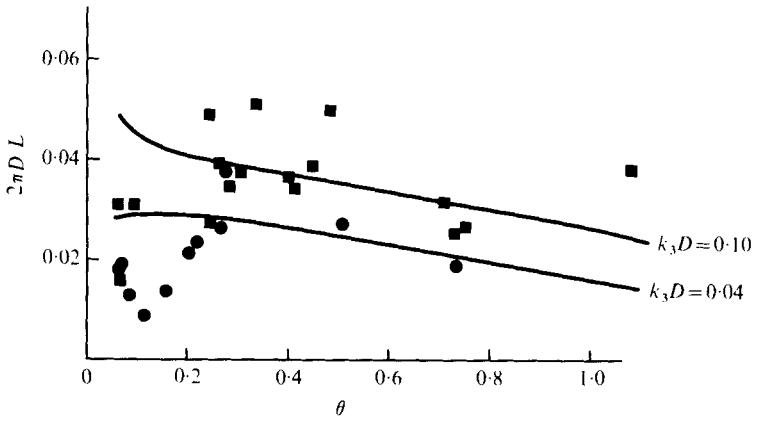

FIGURE 8. Comparison of predicted and longitudinal wavelength of meanders. The unperturbed bed is assumed to be plane. The data are taken from Chang *et al.* (1971). $s = 2{\cdot}65$, $D/d = 1000$ and $c_D = 7$. ●, $k_3 D < 0{\cdot}1$; ■, $k_3 D > 0{\cdot}1$.

must be expected to exist (Engelund & Fredsøe 1974). These data concern meandering as well as braiding, and it is seen that figure 6 describes this transition rather well. The rest of their data, together with other suitable laboratory data, have been plotted in figure 4, assuming the unperturbed bed to be dunes. In the analysis of data, the braided data reported by Leopold & Wolman (1957) have been omitted, as they were obtained in the antidune region, where little is known about the hydraulic resistance. The antidune region is not important in practice.

A special comment is needed on the experiments by Shen & Komura (1968). These were performed in a channel whose width–depth ratio was about 10 while the value of θ was about 0·4, and it was possible to obtain meandering only if they, artificially, made the channel walls very rough. In figure 4 their data for smooth walls are depicted and it is seen that they fall mainly in the stable region. However, by introducing rough walls, the turbulence intensity is increased, which may involve an increase in the ratio q_s/q_b. As we obtain the same tendency by increasing θ in the present theory, their experiments can be explained from figure 4: by increasing θ (or the ratio q_s/q_b), keeping $k_3 D \sim 0{\cdot}30$, we enter the unstable region, where meandering will actually take place.

In figure 4 data from natural rivers have been plotted. If possible, measurements describing bank-full discharge were employed; otherwise instantaneous data were used.

It is seen that, contrary to laboratory measurements, the values of θ in natural rivers are often larger than one. If the suspended sediment were neglected, the theory would predict stability in this case (as seen from figure 5). This would imply that the rivers with large water discharge rates would be straightened up, contrary to all observations.

Meander lengths measured in the laboratory are compared with those predicted by the stability theory in figures 7 and 8. At small values of θ the theory predicts a greater dimensionless wavenumber in the case of a dune-covered bed than for a plane bed. This tendency is partly confirmed by the measurements by Ashnida & Narai (1969), who also indicated in their paper that the bed was dune-covered. As far as the measurements by Ackers & Charlton (1970) and by Schumm & Khan (1972) are

concerned, the deviation from the theory is perhaps due to the bed being covered by ripples rather than by dunes. However, in general the agreement between theory and measurements is satisfactory as the order of magnitude is correct.

In natural rivers the value of θ corresponding to bank-full discharge is often close to unity. It is interesting to note that for such large values of θ the ratio between the longitudinal and transverse wavenumbers approaches values varying from 0·40 for wide rivers ($k_3 D \sim 0{\cdot}04$) to 0·15 for narrow rivers ($k_3 D \sim 0{\cdot}20$). This results in the following range of the ratio of meander length to river width:

$$L/B = \begin{cases} 5 \text{ for wide rivers } (D/B \sim 0{\cdot}01), \\ 14 \text{ for narrow rivers } (D/B \sim 0{\cdot}05). \end{cases}$$

In the data given by Leopold & Wolman concerning rivers in India and America almost all ratios of meander length to river width lie in the interval $5 < L/B < 15$. A more complete comparison between data and theory is difficult, as the water depths are not indicated in their paper.

8. Conclusion

A stability theory has been developed which predicts whether a river meanders, braids or remains straight. By taking into account the effect of the transverse slope in a correct manner and including a description of the behaviour of the suspended sediment, the theory gives results in agreement with experimental findings, namely that a river will always remain straight if its width is smaller than 8 times its depth. Further, the river will braid if its width is larger than about 60 times its depth. The above-mentioned values are slightly dependent on the value of the Shields parameter as shown in figure 4.

The theory predicts a meander length such that at a large value of the Shields parameter a narrow river has a ratio of meander length to river width of about 15, while wide rivers correspond to a smaller ratio of about 5.

No excessive constants have been introduced or fitted in the present theory.

The present work must be regarded as an extension and improvement of the work by Hansen (1967) and Engelund & Skovgaard (1973), carried out at the same institute as the present study. The author is especially grateful to Professor Engelund, who played an important part in the preparation of the present paper.

REFERENCES

Ackers, P. & Charlton, F. G. 1970 The slope and resistance of small meandering channels. *Inst. Civil Engrs, Proc. Suppl.* paper 7362 S.

Ashnida, K. & Narai, S. 1969 The structure of movable bed configuration. *Bull. Disaster Prevention Res. Inst., Kyoto Univ., Kyoto, Japan* **19**, 15–30.

Bagnold, R. A. 1954 Experiments on a gravity-free dispersion of large solid spheres in a Newtonian fluid under shear. *Proc. Roy. Soc.* A **225**, 49.

Callander, R. A. 1969 Instability and river channels. *J. Fluid Mech.* **36**, 465.

Chang, H.-Y., Simons, D. B. & Woolhiser, D. A. 1971 Flume experiments on alternate bar formation. *J. Waterways, Proc. A.S.C.E.* **97** (WW 1), 155.

EINSTEIN, H. A. 1950 The bed-load function for sediment transport in open channel flows. *U.S. Dept. Agric. Tech. Bull.* no. 1026.

EINSTEIN, H. A. & BARBAROSSA, N. L. 1951 River channel roughness. *J. Hyd. Div. A.S.C.E.* **77**, 78.

ENGELUND, F. 1971 Instability of erodible beds. *J. Fluid Mech.* **42**, 225.

ENGELUND, F. 1974 Flow and bed topography in channel bends. *J. Hyd. Div. A.S.C.E.* **100** (HY 11), 1631.

ENGELUND, F. 1975 Instability of flow in curved alluvial channels. *J. Fluid Mech.* **72**, 145.

ENGELUND, F. & FREDSØE, J. 1974 Transition from dunes to plane bed in alluvial channels. *I.S.V.A., Tech. Univ. Denmark Series Paper* no. 4.

ENGELUND, F. & FREDSØE, J. 1976 A sediment transport model for straight alluvial channels. *Nordic Hydrologi* **7**, 293.

ENGELUND, F. & HANSEN, E. 1972 *A Monograph on Sediment Transport in Alluvial Streams.* Copenhagen: Technical Press.

ENGELUND, F. & SKOVGAARD, O. 1973 On the origin of meandering and braiding in alluvial streams. *J. Fluid Mech.* **57**, 289.

FERNANDÉZ LUQUE, R. 1974 Erosion and transport of bed sediment (Diss.). *Krips Repro B.V.-Meppel.*

FREDSØE, J. 1976 Levelling of side slopes in river navigation channels. *I.S.V.A., Tech. Univ. Denmark Prog. Rep.* no. 38.

FREDSØE, J. & ENGELUND, F. 1975 Bed configurations in open and closed alluvial channels. *I.S.V.A., Tech. Univ. Denmark Series Paper* no. 8.

FRIEDKIN, J. F. 1945 A laboratory study of the meandering of alluvial rivers. *Rep. U.S. Waterways Exp. Station, Vicksburg, Mississippi.*

GOTTLIEB, L. 1976 Three-dimensional flow pattern and bed topography in meandering channels. *I.S.V.A., Tech. Univ. Denmark Series Paper* no. 11.

HANSEN, E. 1967 The formation of meanders as a stability problem. *Hydraul. Lab., Tech. Univ. Denmark Basic Res. Prog. Rep.* no. 13.

HUBBEL, D. W. & MATEJKA, D. Q. 1959 Investigations of sediment transportation. Middle Loup River at Dunning, Nebraska. *Geol. Survey Water-Supply Paper* no. 1476.

LEOPOLD, L. B. & WOLMAN, M. G. 1957 River channel patterns: braided, meandering and straight. *Geol. Survey Prof. Paper* no. 282-B.

PARKER, G. 1976 On the cause and characteristic scales of meandering and braiding in rivers. *J. Fluid Mech.* **76**, 457.

ROUSE, H. 1937 Modern conceptions of the mechanics of turbulence. *Trans. A.S.C.E.* **102**, 463.

SCHUMM, S. A. 1969 River metamorphosis. *J. Hyd. Div. A.S.C.E.* **95** (HY 1), 255.

SCHUMM, S. A. & KHAN, H. R. 1972 Experimental study of channel pattern. *Geol. Soc. Am. Bull.* **88**, 1755.

SHEN, H. W. & KOMURA, S. 1968 Meandering tendencies in straight alluvial channels. *J. Hyd. Div. A.S.C.E.* **94** (HY 4), 997.

YALIN, M. S. 1972 *Mechanics of Sediment Transport.* Pergamon.